

M-Blocks: Momentum-driven, Magnetic Modular Robots

John W. Romanishin, Kyle Gilpin and Daniela Rus

Abstract—In this paper, we describe a novel self-assembling, self-reconfiguring cubic robot that uses pivoting motions to change its intended geometry. Each individual module can pivot to move linearly on a substrate of stationary modules. The modules can use the same operation to perform convex and concave transitions to change planes. Each module can also move independently to traverse planar unstructured environments. The modules achieve these movements by quickly transferring angular momentum accumulated in a self-contained flywheel to the body of the robot. The system provides a simplified realization of the modular actions required by the sliding cube model using pivoting. We describe the principles, the unit-module hardware, and extensive experiments with a system of eight modules.

I. INTRODUCTION

We wish to create robotic systems capable of autonomously changing shape in order to match the system's structure to the task at hand. Many interesting robotic systems have been proposed in pursuit of this goal [1]. This paper describes a new unit module, the M-Block, a magnetically-bonded, angular momentum-actuated modular robot. These 50 mm cubes are autonomous robots that have no external actuated moving parts, and no tethers. The modules realize pivoting using inertial force actuation. A flywheel located inside the module, (oriented in the plane of the intended motion), is used to store angular momentum before a braking mechanism is used to decelerate the flywheel and, during a short duration, exert a high torque on the module. If this torque is sufficiently high, the module breaks its magnetic bonds with its neighbors and pivots into a new location. Because the modules use passive connectors, they could be hermetically sealed, making them extremely robust to harsh environmental conditions.

An individual module can move autonomously in an unstructured environment using this pivoting (rolling) locomotion. A module can also move on a 3D lattice of identical modules, achieving a desired trajectory on a planar surface or making convex and concave transitions to other planes. The modules can also jump over distances up to several body widths wide. This broad range of motions enables the M-Block system to achieve a wide range of shape changing and locomotion capabilities.

Similar to the sliding cube model (SCM) [2], we define a pivoting cube model (PCM). The PCM defines the types of movements that the M-Blocks can execute in the process of transitioning from one configuration to another. The SCM has been a mainstay of the modular robotics field,

J. W. Romanishin, K. Gilpin and D. Rus are with the Computer Science and Artificial Intelligence Lab, MIT, Cambridge, MA, 02139 {johnrom|kwegilpin|rus}@csail.mit.edu.

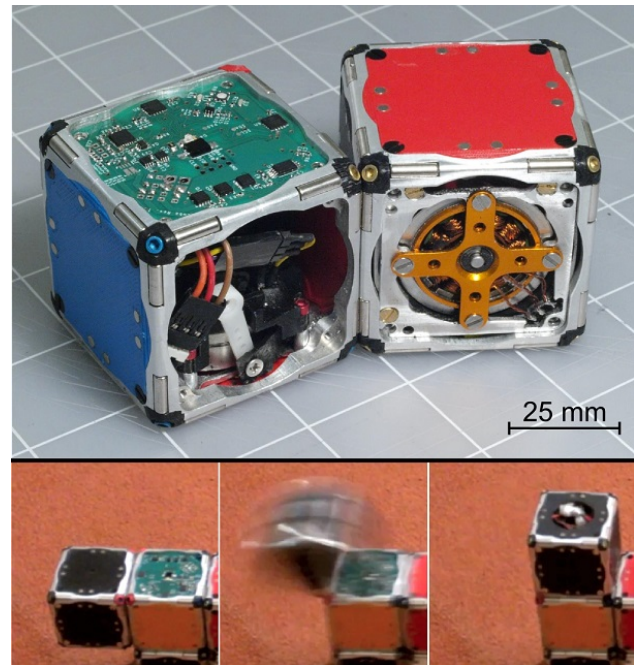


Fig. 1: Neighboring M-Blocks bond through permanent magnets embedded in their edges while additional magnets on their faces help with alignment. The modules locomote by pivoting about any of their twelve edges which allows for a variety of movements, including the convex transition shown here. All movements are driven by a torque generated by rapidly decelerating an internal flywheel. (The two large modules are pictured on a one-inch grid.)

both supporting theoretical developments and driving new hardware instantiations. Given a group of homogeneous, typically cubic modules, the SCM posits that a given module can perform a planar traversal from one of its neighboring modules to an adjacent module. While the SCM has proven to be a convenient framework for theoretical work [2], physical realizations of modules that can actually implement the SCM have been limited. We know of no hardware which can reliably implement the SCM in three dimensions. Hardware systems which implement the SCM in two dimensions are often mechanically complex and prone to failure.

While research in chain-based modular robots is quite active [3], [4], focus has shifted away from lattice-based approaches based on the SCM model. If we expect lattice-based self-reconfigurable systems to remain an active area of research, we should move past the sliding cube model and all of its practical limitations. This paper makes a number of contributions to this end. First, the pivoting cube model that it presents is theoretically attractive. While the PCM is not equivalent to the SCM, the PCM still allows generic

self-reconfiguration, and it enables some types of motions that are not supported under the SCM. Second, the M-Block hardware that we present relies on simple principles that eliminate the mechanical complexities of many existing systems. Finally, the experimental hardware characterization provided in this paper demonstrates that self-reconfiguration through pivoting with inertial forces is practical and could be a viable basis for a system containing hundreds of modules.

The remainder of this paper is organized as follows. Section II gives an overview of related work that pertains to the M-Blocks system. Section III presents the hardware design of the modules. Section IV then presents the pivoting cube model and illustrates the types of movements that it supports. Next, Section V presents data characterizing the hardware and the results of many experiments with the system. Finally, Section VI concludes with a short discussion and ideas for future work.

II. RELATED WORK

We situate our work with respect to other cubic lattice-based modular robotic systems [1]. Self-reconfiguring lattice-based modular robots can be broadly categorized by two attributes: the mode of locomotion and the connection mechanism. Perhaps the most elegant model for locomotion is termed the sliding cube model [2]. In this model, cubes translate (i.e. slide) from one lattice position to another. Despite its theoretical simplicity, we know of no hardware which implements this approach in the general 3D case. We do know of two systems [5], [6] which implement a 2D version of the sliding cube model in the vertical plane and two systems [7], [8] that operate horizontally. Not only are all of these systems mechanically complex, it is not clear how any of these systems could be extended to 3D.

A common alternative to the sliding cube model is rotating one or more connected modules about a pivot point that is on a face or inside of a module [9], [10], [11], [12], [13]. The I-Cubes [14] use 3-DOF linkages to reconfigure passive modules in a cubic lattice. Another approach to locomotion relies on modules that expand and contract in either two [15] or three [16] dimensions. Other systems [17] employ modules which can more generally deform.

Our work is most closely related to existing systems whose modules pivot about the edges they share with their neighbors [18], [19], [20]. These existing pivoting systems are confined to the horizontal plane and use complex connection mechanisms and/or external actuation mechanisms to achieve reconfiguration. These prior works make no attempt to define a generalized, three-dimensional model for reconfiguration through pivoting. This paper will present a physical pivoting cube model that can be applied to both solitary modules and groups acting in synchrony. Our model captures physical quantities including mass, inertia, and bonding forces.

The other defining characteristic of any modular robotic system is its connectors. Many modular systems use mechanical latches to connect neighboring modules [14], [9], [15]. Mechanical latches typically suffer from mechanical complexity and an inability to handle misalignment. Other

systems such as the Catoms [21], Molecule [10], and EM-Cube [8] use electromagnets for inter-module connections. Electromagnets consume more power and are not as strong as mechanical latches. Electropermanent magnets [22] are an attractive alternative because they only consume power when changing state, but they still require high instantaneous currents to actuate and are not readily available. One unique system [23] uses fluid forces to join neighboring modules, but must operate while submerged in viscous fluid. Another, the Catoms [24], uses electrostatic forces for bonding. The unifying feature of all of these connection mechanisms is that their holding force can be controlled: on, off, or somewhere in-between. This adds complexity and decreases robustness.

In contrast to all of the systems just mentioned, M-Blocks use a simple mode of locomotion (pivoting), a simple inertial actuator (a flywheel and brake), and a simple bonding mechanism (permanent magnets). Actuation through inertial control has been used extensively in space [25] and underwater robotics [26] as well as several earth-bound applications [27]. We know of only one modular robotic system, the XBot [20], that uses the inertia of the modules to induce pivoting, but the necessary forces are applied externally; the system is only two-dimensional; and the modules are constrained to 180 degree rotations. The simplicity of the M-Blocks, with their self-contained inertial actuators, allows our system to achieve both robust self-reconfiguration and independent locomotion in 3D environments.

III. HARDWARE

We have constructed four first generation M-Block robots, along with four un-actuated modules. As shown in Figure 1, each 143 g module is constructed from a 50 mm cubic frame milled from a single piece of 7075 aluminum and the module, (including the flywheel), has a moment of inertia, about the center of mass, of $63.0\text{E-}6 \text{ kg m}^2$. This frame holds twenty-four cylindrical bonding magnets along its twelve edges. Six bolt-on panels contain various electrical and mechanical elements such as the inertial actuator and the control PCB. Additionally, each of these panels is inset with eight outward-facing magnets that assist in alignment between neighboring modules. The active modules are equipped with on-board power, computation, actuation, and communication capabilities (see Figure 2(a)). They can move on a structure formed by the passive modules (which still have all necessary magnets) or completely independently over open ground.

Cost and robustness of modular robots become limiting factors when producing modular systems with many modules. The M-Blocks attempt to address these issues due to their mechanical simplicity and limited number of moving parts. The per unit cost of the five modules that were produced was \$260, but this did not include machining costs, which would have been substantial. (We estimate that in quantity 100 the per unit cost, including all machining, would be \$200.) The remainder of this section provides a detailed look at the design of the three critical systems inside each robot: the magnetic bonding and pivoting mechanism; the inertial actuator, and the electronic control system.

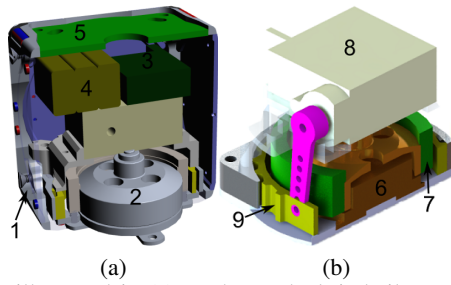


Fig. 2: As illustrated in (a), each M-Block is built around a solid aluminum frame (1) and contains an inertial actuator (2), a motor controller (3), batteries (4), and control circuitry (5). The inertial actuator is detailed in (b). It is composed of a brushless DC motor (6) which spins a flywheel (7). A servo motor (8) is used to tighten a belt (9) which rapidly decelerates the flywheel to create an impulse of torque.

A. Magnetic Edge and Face Bonds

An important aspect of the M-Block system is the novel design that allows the modules to quickly form magnetic, non-gendered, hinges on any of the cubes' twelve edges. These hinges must provide enough force to maintain a pivot axis through various motions. The design solves this challenge by using twenty-four diametrically polarized cylindrical magnets, two of which are situated coaxially with each edge of the frame. The diametrically magnetized cylinder magnets are free to rotate as shown by the arrows in Figure 3. This rotation allows configurations with two, three, or four modules to form structural magnetic bonds.

The magnets are set back from the corners of each cube as shown in Figure 4. This set-back is critical to the M-Block system performance because it guarantees that the strength of a hinge bond between two modules (involving four total magnets) is not dwarfed by the strength of the face bond between two modules (involving sixteen total magnets) when the modules are flush and well aligned. In contrast, if the face bonds were much stronger than the hinge bonds, the energy provided by the inertial actuators to break the face-to-face bond would overpower the hinge bond and result in the active module careening away from the assembly.

While the edge magnets form strong hinges and serve to connect neighboring modules in the lattice, they are not sufficient to overcome misalignments that are introduced when modules pivot. To solve the alignment problem, we embedded eight 2.5 mm diameter disc magnets in each of the six faces. These disc magnets are arranged in an eight-way symmetric pattern in order to maintain the modules' gender neutrality. These alignment magnets are strong enough to pull a module into alignment as it finishes a rotation, but they do not add significant holding force to the face bonds.

B. Inertial Actuator

In order for a module to overcome the forces of the magnetic bonding system, it needs to provide a torque for a relatively short time period. As illustrated in Figure 2(a,b), our actuator is a unidirectional reaction wheel designed to release all of its energy in less than 15 ms, thereby creating

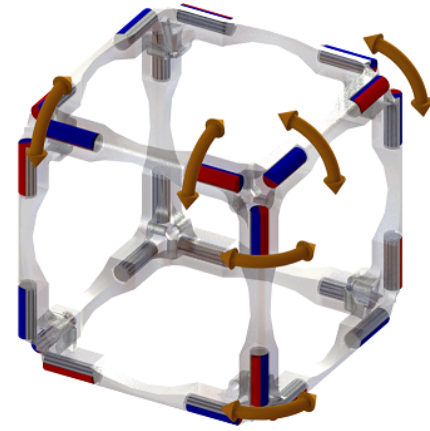


Fig. 3: Each cube frame (translucent) holds twenty-four diametrically polarized magnets in its edges that are free to rotate as shown by the orange arrows. This configuration allows the cubes to form face or hinge bonds.

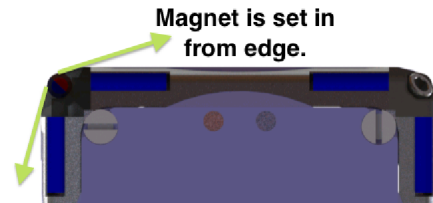


Fig. 4: The two magnets in all edges of each cube are set back from the corners by 1 mm. This air gap decreases the strength of the planar bonds (which involve eight magnets per cube) so that its does not overwhelm the strength of the hinge bonds (which only involve two magnets per cube).

an approximate impulse of torque. The flywheel itself is a 20g stainless steel ring with a moment of inertia of $5.5E-6 \text{ kg m}^2$. It is fixed to an out-runner style brushless DC motor that is capable of spinning at up to 20000 rpm.

We quickly decelerate the flywheel with a self-tightening rubber belt that is wrapped around the flywheel's circumference. When un-actuated, the belt is loose and constrained by a cage to maintain clearance from the flywheel (see Figure 5(a)). To tighten the belt and stop the flywheel, we use a hobby-style servo motor which pulls the belt in the single allowable direction of rotation (see Figure 5(b)). As the belt contacts the flywheel, the flywheel's motion further tightens the belt resulting in a rapid deceleration.

C. Electronics

Each module is controlled by a custom-designed PCB which includes a 32-bit ARM microprocessor and a 802.11.4 XBee radio from Digi International. Three 3.7 V, 125 mAh LiPo batteries connected in series power the modules. The processor responds to commands received from a remote XBee device connected to the user's computer in order to control the inertial actuator. The low-level BLDC control is performed by a commercial motor driver. Because the BLDC driver provides no feedback to the microprocessor, we employ a photo-reflector to measure the speed of a striped encoder disk attached to the flywheel. Additionally, each PCB

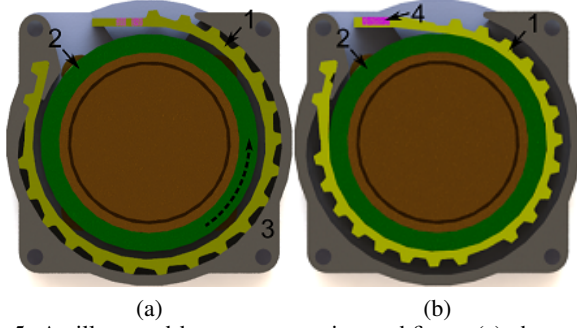


Fig. 5: As illustrated by a cutaway view, subfigure (a) shows how a rubber belt (1), is used to rapidly decelerate the flywheel (2). When un-actuated, the belt rests against a cage (3), away from the flywheel. Subfigure (b) illustrates how, when the belt is tightened by a servo (4), it is pulled in the same direction that the flywheel is spinning so that the belt self-tightens. Due to the design of the mechanism, it can only brake the flywheel when the flywheel is spinning in the direction indicated by the dashed arrow.

includes a 6-axis IMU (to determine absolute orientation); an outward-facing IR LED/photodiode pair (for neighbor-to-neighbor communication); and several Hall effect sensors (to detect misalignment between modules).

IV. PIVOTING CUBE MODEL

A. Pivoting Cube Model Theory

The sliding cube model (SCM) is one of the more prevalent algorithmic frameworks that has been developed for modeling the motions of lattice based self-reconfiguring modular robots. To overcome the physical implementation issues of the sliding cube model and to utilize the favorable traits of the M-Block hardware presented in Section III, we develop a new physical pivoting cube model (PCM) that is inspired by existing theoretical models [28]. In our PCM, cubic modules locomote by pivoting about their edges, in effect rolling from one position to the next. While the specifics of the approach differ from those of the SCM, pivoting still allows generalized reconfiguration.

Our model includes several assumptions about the types of motions the modules can execute:

- While already assumed by other models [28], the modules involved in pivoting motions sweep out a volume that must not intersect other modules. Figure 6a.
- Stable lattice configurations must have modules connected via their faces, not their edges. (This is in contrast to other models [28].) Figure 6b.
- Modules involved in pivoting motions must be able to slide past stationary modules in adjacent planes. Figure 6c.
- Modules can locomote in unstructured environments without a supporting lattice, (e.g. on the ground).
- Multiple modules can move as a connected unit, but they must all share a single axis of rotation.

These assumptions allow individual modules or groups of modules to execute a range of motions including concave transitions, convex transitions, and translations (both on and

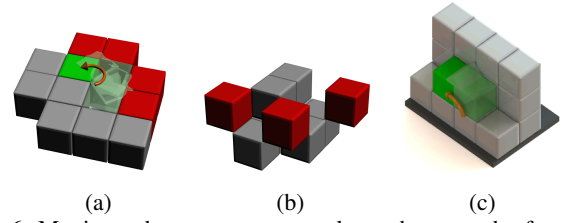


Fig. 6: Moving cubes sweep out a volume that must be free from other cubes in order to allow motions (a). Although cube edges bond to each other - due to edge geometry any cube attached only through edge bonds (shown in red) is not part of the regular lattice configuration (b). Faces have no protruding elements allowing cubes to slide past each other, although friction can be significant (c).

off lattice). In particular, a disjoint set of modules can locomote over open ground to coalesce at a centralized point and then proceed to form an arbitrary structure. To complement our model's theoretical underpinnings, we supplement it with realistic physical constraints. These include mass, inertia, gravity, friction, etc., but we assume that the modules are rigid bodies and that the pivot axes do not slip.

In the most basic instantiation, a pure moment ($T_{pm}^{(k)}$) is applied to the k -th module by its inertial actuator. This moment would cause an unconstrained module to rotate about its center of gravity, but the geometric constraints instead force the module to rotate about a pivot axis that is created by the magnet hinge (see Figure 7). Using the parallel axis theorem, we can calculate the moment of inertia about this pivot axis. This approach can be generalized to find the moment of inertia (I_A) for any set (A) of connected modules about an arbitrary axis. Because the actuators generate pure moments, all of their applied torques can be superimposed and applied en masse about the assembly's pivot axis.

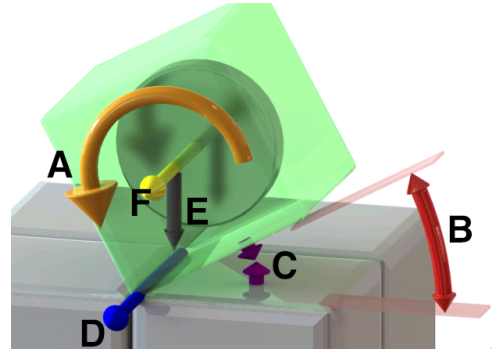


Fig. 7: When a torque (A) about an axis (F) causes the module to pivot through an angle θ (B) about an axis (D), the modules experience additional forces: downward force due to gravity (E) and magnetic force from the face-to-face bonds and any edge bonds being broken (C).

Other forces, including gravity ($m_A \cdot g$), generalized magnetic forces ($F_m^{(k)}$), and friction act to prevent this pivoting (see Figure 7). If the single module in Figure 7 is viewed as a generalized set of modules moving as a rigid unit, one can construct a torque balance equation for the assembly:

$$\frac{d^2\theta}{dt^2} = \frac{-m_A \cdot g \cdot \cos(\theta) \cdot r_{cg} + \sum_{k \in A} T_{pm}^{(k)}(t) - F_m^{(k)}(\theta) \cdot r^{(k)}}{I_A}$$

While not explicitly stated in the equation, θ is a function of time. r_{cg} is the distance between the pivot axis and the assembly's center of gravity, and $r^{(k)}$ is the distance between the pivot and the center of the face of the k -th module in the assembly. This differential equation is non-linear and time-varying. It ignores sliding friction which would be subtracted from the numerator of the right-hand side (thereby resisting the torque of the actuators) and which will be highly dependent on the configuration of modules in adjacent planes. Solving this equation for $\theta(t)$ would give us an approximate description of the motion of a set of modules. We used this equation as a basis for a rough analysis and comparison of the different physical parameters and torques acting on the system.

The basic message of the equation is that one should aim to maximize pure moments ($T_{pm}^{(k)}$) while minimizing the mass (m_A) and inertia (I_A). While decreasing the magnetic bonding strengths ($F_m^{(k)}$) would lead to more energetic motions, those same magnetic forces are used to maintain the magnetic hinges and the system's structural integrity. Finally, it is worth emphasizing that the pure moments from all of the inertial actuators sum equally over all the modules in a rigid assembly. This is a fundamental property of inertial forces and allows multiple modules to move as a group.

B. Autonomous Motion

In order for modular robots to realize self-assembly and robust operation, the unit modules need to be both self-contained and independently mobile. Although researchers have produced modular systems in which the modules can locomote independently, most of these systems are limited to controlled environments [3], [12]. In contrast, the M-Blocks are independently mobile, and they show an ability to move through difficult environments. Although they only have a single actuator, they can exhibit several motions including rolling, spinning in place, and jumping over obstacles up to twice their height.

This diverse set of motion primitives enables novel motion algorithms. One method that we use to drive an M-Block towards a specific goal is to implement a bimodal behavior. When the module's actuator is aligned with the goal location, the actuator is used to apply a moderate amount of torque that causes controlled rotation toward the goal. When the module is not aligned with the goal, we stochastically reorient the module using a high torque that causes unpredictable movement. A group of disjoint M-Blocks executing this behavior can self-assemble into a lattice structure.

C. Lattice Reconfiguration

Once a group of M-Blocks has aggregated into a lattice structure, the modules are able to reconfigure using a variety of motion primitives. For an example of lattice

reconfiguration, see Figure 8(a-d). In general, the modules can execute translations, convex transitions, and concave transitions. When translating, the modules rotate through 90 degrees to move to an adjacent position within the same plane. Translations can be vertical (ascending or descending) or horizontal (supported from any side, including above). For examples of translations, see columns 1–3 of Table I.

Convex and concave transitions allow the modules to move between orthogonal planes. Convex transitions are used to traverse outside corners by rotating through 180 degrees. We have shown that the modules can perform convex transitions in either horizontal or vertical planes (columns 4–5 of Table I). Concave transitions are 90 degree rotations that are used to traverse inside corners. As before, these moves can be horizontal or vertical (columns 6–7 of Table I). Due to the fact that the active module is bonded to neighbors in two orthogonal planes when the move begins, we have found that the torque required to execute concave transitions approaches the limits of what our actuators can provide. (Future version of the system will employ a number of mechanisms to overcome this limitation.)

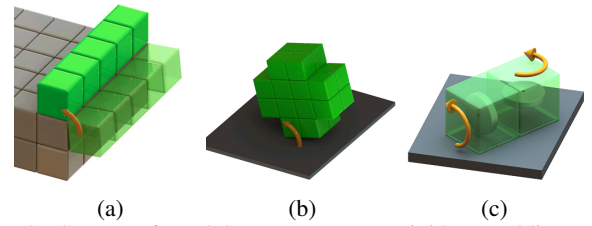


Fig. 9: Groups of modules can move as rigid assemblies. Two-dimensional movements can be extended along the pivoting axis (a). Modules can aggregate and roll as an assembly (b). A few M-Blocks with orthogonal actuators can form easily controllable meta-modules (c).

D. Group Movement

When operating on a lattice, groups of modules that share the same pivot axis are able to coordinate their actuators in order to move together. Not only does this increase the stability of the motion due to longer pivots as in Figure 9(a), but it also decreases planning complexity when attempting to relocate groups of modules on a lattice.

Assemblies of modules are able to move together in the environment by first reconfiguring in order to approximate a wheel or sphere (Figure 9(b)) and then simultaneously applying their inertial actuators. An additional type of group movement involves small groups forming meta-modules (Figure 9(c)) to more precisely control their trajectories. The modules can be oriented such that their actuators are aligned in orthogonal planes allowing control over additional degrees of freedom. When a disjoint group of modules is self-assembling, these meta-modules can serve as intermediate assemblies to increase the speed of the aggregation.

V. EXPERIMENTS

We characterized the M-Block hardware, and we performed experiments with lattice-reconfigurations and group

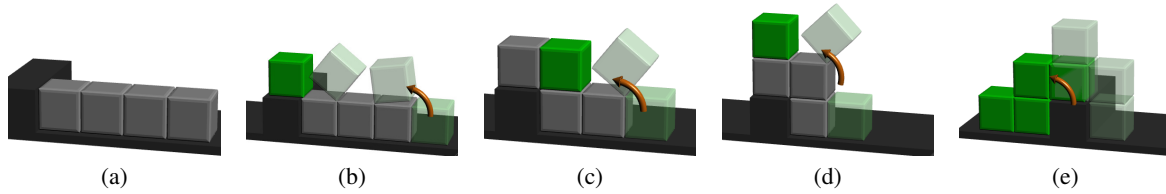


Fig. 8: These five frames show a modeled progression of a group of four modules that encounter and attempt to traverse an obstacle. They first reconfigure into a tall shape in order to move the center of gravity of the group as far towards the direction of travel as possible. After they have achieved this, in part e, all of the modules simultaneously apply moments to pivot the whole group over the obstacle.

movements. We tested the modules as they executed a range of different lattice reconfiguration moves; a representative sample of these moves is shown in Table I. Additionally, video frames taken from the video linked in the supplementary materials are shown in Figure 12.

A. Characterizing the Actuator

Each M-Block inertial actuator needs to provide a high, almost instantaneous, application of torque in order to break the strong permanent magnet bonds. As previously described, the actuator is able to decelerate the flywheel from 2100 to 0 rad/s in about 15 ms. By differentiating the measured angular velocity profile of the flywheel during deceleration, we have estimated the torque as shown in Figure 10. The entire actuation event, from the moment the brake signal is sent, to moment when the flywheel reaches zero angular velocity, is roughly 50 ms. The torque peaks at about 1.25 Nm. As shown in Figure 10, most of the torque is applied over a 15 ms span, which transfers approximately 600 watts (average) to the cube frame. In experiments with several different modules, we have noticed that the maximum applied torque varies with the particular actuator due to belt wear and flywheel material.

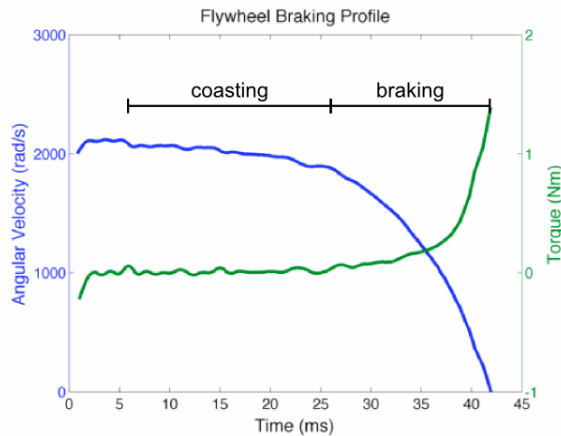


Fig. 10: This graph shows the angular velocity profile of the inertial actuator's flywheel as measured by an optical encoder. The torque was found by differentiating this motion and applying the relevant physical parameters. The peak torque that the actuator provides is on the order of 1.25 Nm.

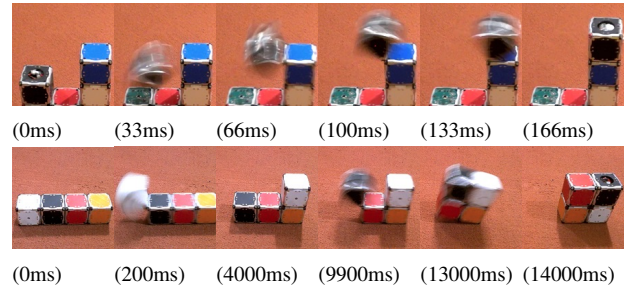


Fig. 12: These video frame sequences show six consecutive frames for a jump motion (a), and six frames for an assembly movement over a span of 14 seconds (b).

B. Characterizing the Magnets

As previously described in Section III the magnet bonding system needs to provide enough force for robust face-to-face connections as well as strong edge-to-edge bonds. To provide this high strength in a small volume, we used N-52 grade rare-earth neodymium magnets. The pull strength of various configurations are shown in Figure 11. The pull strength of about 23 N is enough to support a chain of 16 modules hanging vertically. Additionally, the torque required to separate two modules (in two different configurations) is shown in Figure 11(c). The high torque exhibited for the module bonded with two neighboring faces is near the limit of what the inertial actuator can overcome. (We are experimenting with bigger flywheels in order to apply more torque.)

C. System Experiments

An important goal of the M-Blocks is to provide robust lattice reconfiguration. Table I demonstrates the results of a range of different attempted motions. The range of flywheel RPM's before braking was found through trial and error. A motion is considered a success if after three attempts the module moves to its desired lattice position. The two most common failure modes were insufficient torque and disconnection from the lattice. Additionally, modules sometimes have too much inertia and overshoot their desired lattice positions. We attribute the insufficient torque failures to several factors: low battery voltage resulting in reduced motor speed; belt and flywheel surface conditions resulting in unpredictable torque profiles; and inherent random variability in the friction between the belt and the flywheel. We attribute the lattice disconnection failures to variability in the bond

TABLE I: This table shows experimental results for controlled tests of various motion primitives. The RPM measurements are approximated using the on-board optical encoder. Some of the motions were performed using experimental upgrades that were not implemented in all of the hardware; the \star indicates a brass flywheel with a higher moment of inertia, and the \dagger indicates the use of gear teeth on the edges for additional friction.

	Traverse	Horizontal Traverse	Vertical Traverse \dagger	Horizontal Convex	Vertical Convex $\dagger \star$	Horizontal Concave \star	Vertical Concave \star	Corner Climb	Jump \star
Illustration									
kRPM	11-13	10-12	16-18	8.5-12	13-15	19-21	16-17	17-18	19-21
Attempts	21	20	20	20	20	20	20	15	55
Successes	91%	75%	60%	80%	70%	65%	70%	93%	51%

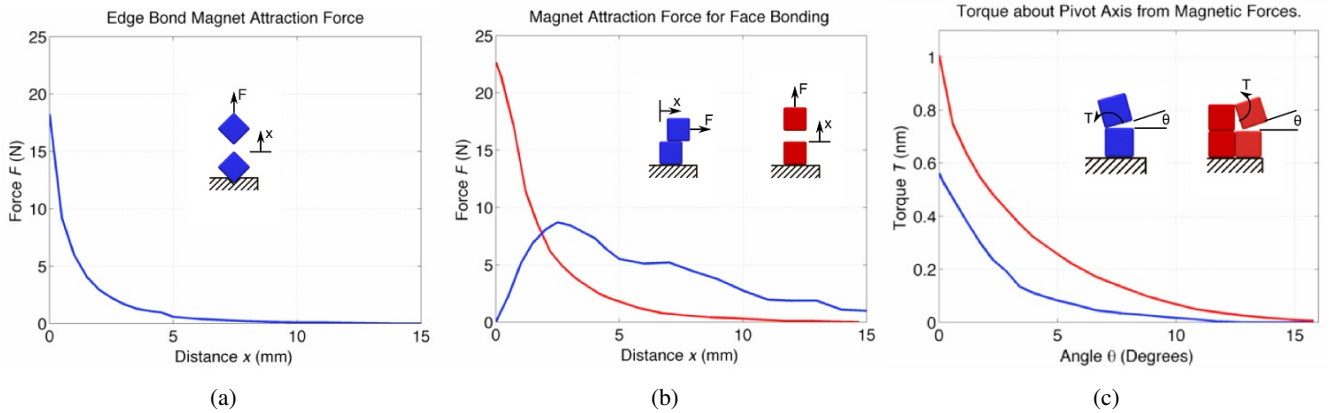


Fig. 11: The force of the hinge strength drops quickly after holding a maximum force of around 18 N (a). The force between the faces in tension (red), and in shear (blue) are important for bonding (b). We measured the torque required to rotate a module as a function of an angle (c). The torque required in the four module configuration approaches the limit of the current actuator.

interactions and slipping of the pivot axis (which prompted us to experiment with gear teeth attached to the cube edges). The bond strengths vary due to manufacturing tolerances, edge magnet state, and module alignment. In particular, debris can accumulate and impede the free rotation of the edge magnets.

We also performed a number of less formal tests involving individual modules and groups of modules moving both on the lattice and in the surrounding environment. We found that a module could execute 20–100 motions before depleting its battery, depending on the difficulty of the motions. Two examples are shown in Figure 12, and more examples can be found in the supplemental video. Figure 12(a) shows a single module jumping a distance that is one module high and two modules wide. Figure 12(b), shows two active modules reconfiguring into a 4-module approximation of a wheel, and then simultaneously apply their actuators in order to roll the whole structure. (Note that, in the last frame, the white module has transitioned from the upper right to the lower right.) Additionally, we have tested that the modules are able to traverse on carpet, brick, and grass at speeds up to 1 m/s.

VI. DISCUSSION

We have introduced the M-Blocks, 50 mm cubic robots that use inertial forces to move independently in a range of environments; perform lattice-reconfigurations on a substrate of identical modules; and move ensembles of modules in both lattice reconfigurations and in external environments. The M-Blocks are relatively simple and robust—attributes essential when scaling a modular robotic system into the hundreds or thousands. There remain several difficulties and limitations of the M-Block system. The modules contain only a one-dimensional, uni-directional inertial actuator. The modules are unable to descend in a controlled fashion and instead continue descending until they encounter a horizontal step. The actuator is not strong enough to execute all lattice moves reliably. There is no intelligence incorporated into the system, so a module cannot self-recover if it fails to successfully execute a particular move.

Future versions of the M-Blocks could be implemented at various scales. The pivoting cube model is scale-independent, and a simplified analysis of the individual modules shows that they are roughly scale independent. The ratio of the actuator inertia to total module inertia remains constant as the modules undergo volumetric scaling. Material considerations dictate that smaller objects can spin faster than large ones, so in theory, smaller flywheels could develop larger torque

to mass ratios. However, assuming constant flywheel speed and volumetric scaling, the torque to volume ratio for a fixed volume of M-Blocks increases as the characteristic module size approaches the fixed volume. That is, a single module of given size will have more torque than a group of smaller modules configured into the same volume. This property affects the system capabilities of assemblies of modules moving together. Other factors such as magnetic strength, energy density, material properties, and manufacturing constraints will likely affect scaling in complex ways.

We are developing a three-dimensional design with a bidirectional flywheel which will allow us expanded control over the actuation torque. We are also considering heterogeneous modules patterned off of the basic M-Block modular architecture that are capable of specific tasks such as supplementary power storage, manipulation, and traditional (e.g. wheel or legged) locomotion methods.

We are also interested in exploring a wide breadth of control and planning algorithms. Due to their natural tendency to self-align, combined with their on-board sensing and independent movement capabilities, we believe that the modules will have the ability to move robustly and correct for errors. An additional algorithmic challenge is deciding how we can best use the modules' inertial actuators to roll a large assembly through an open environment. We are hopeful that the contributions we have presented here, combined with additional refinements, will result in a lattice-based modular robotic system that is robust, simple to use, and highly capable.

ACKNOWLEDGEMENTS

This work is supported by the NSF through grants 1240383 and 1138967. The authors would like to thank the Eloranta fellowship for its initial support, Ron Wiken in the CSAIL machine shop, Andy Marchese, and Ross Knepper.

SUPPLEMENTARY MATERIAL

<http://youtu.be/mOqjFa4RskA>

REFERENCES

- [1] M. Yim, W. Shen, B. Salemi, D. Rus, M. Moll, H. Lipson, E. Klavins, and G. S. Chirikjian, "Modular Self-Reconfigurable Robot Systems: Challenges and Opportunities for the Future," *Robotics and Automation Magazine*, vol. 14, no. 1, pp. 43–52, 2007.
- [2] R. Fitch, Z. Butler, and D. Rus, "Reconfiguration planning for heterogeneous self-reconfiguring robots," in *Intelligent Robots and Systems*, 2003, pp. 2460–2467.
- [3] J. Davey, N. Kwok, and M. Yim, "Emulating self-reconfigurable robots - design of the smores system," in *Intelligent Robots and Systems*, 2012, pp. 4464–4469.
- [4] T. Han, N. Ranasinghe, L. Barrios, and W.-M. Shen, "An online gait adaptation with superbot in sloped terrains," in *International Conference on Robotics and Biomimetics (ROBIO)*, December 2012.
- [5] K. Hosokawa, T. Tsujimori, T. Fujii, H. Kaetsu, H. Asama, Y. Kuroda, and I. Endo, "Self-organizing collective robots with morphogenesis in a vertical plane," in *International Conference on Robotics and Automation*, 1998, pp. 2858–2863.
- [6] Y. Suzuki, N. Inou, H. Kimura, and M. Koseki, "Reconfigurable group robots adaptively transforming a mechanical structure," in *Intelligent Robots and Systems*, 2008, pp. 877–882.
- [7] C. Chiang and G. S. Chirikjian, "Modular Robot Motion Planning Using Similarity Metrics," *Autonomous Robots*, vol. 10, pp. 91–106, 2001.
- [8] B. K. An, "Em-cube: Cube-shaped, self-reconfigurable robots sliding on structure surfaces," in *IEEE International Conference on Robotics and Automation (ICRA)*, May 2008, pp. 3149–3155.
- [9] H. Kurokawa, S. Murata, E. Yoshida, K. Tomita, and S. Kokaji, "A 3-d self-reconfigurable structure and experiments," in *Intelligent Robots and Systems*, October 1998, pp. 860–865.
- [10] K. Kotay and D. Rus, "Locomotion versatility through self-reconfiguration," *Robotics and Autonomous Systems*, vol. 26, no. 2–3, pp. 217–232, 1999.
- [11] D. Brandt and D. J. Christensen, "A new meta-module for controlling large sheets of ATRON modules," in *Intelligent Robots and Systems*, October 2007, pp. 2375–2380.
- [12] M. D. Kutzer, M. S. Moses, C. Y. Brown, D. H. Scheidt, G. S. Chirikjian, and M. Armand, "Design of a new independently-mobile reconfigurable modular robot," in *International Conference on Robotics and Automation*, 2010, pp. 2758–2764.
- [13] Y. Meng, Y. Zhang, A. Sampath, Y. Jin, and B. Sendhoff, "Cross-ball: A new morphogenetic self-reconfigurable modular robot," in *IEEE International Conference on Robotics and Automation (ICRA)*, May 2011, pp. 267–272.
- [14] C. Ünsal and P. K. Khosla, "Mechatronic design of a modular self-reconfiguring robotic system," in *IEEE International Conference on Robotics and Automation (ICRA)*, April 2000, pp. 1742–1747.
- [15] D. Rus and M. Vona, "Crystalline robots: Self-reconfiguration with compressible unit modules," *International Journal of Robotics Research*, vol. 22, no. 9, pp. 699–715, 2003.
- [16] J. W. Suh, S. B. Homans, and M. Yim, "Telecubes: Mechanical design of a module for self-reconfigurable robotics," in *International Conference on Robotics and Automation*, May 2002, pp. 4095–4101.
- [17] A. Pamecha, I. Ebert-Uphoff, and G. S. Chirikjian, "Useful metrics for modular robot motion planning," *Transactions on Robotics and Automation*, vol. 13, no. 4, pp. 531–45, 1997.
- [18] S. Murata, H. Kurokawa, and S. Kokaji, "Self-assembling machine," in *IEEE International Conference on Robotics and Automation (ICRA)*, 1994, pp. 441–448.
- [19] E. Yoshida, S. Murata, S. Kokaji, A. Kamimura, K. Tomita, and H. Kurokawa, "Get back in shape! a hardware prototype self-reconfigurable modular microrobot that uses shape memory alloy," *Robotics and Automation Magazine*, vol. 9, no. 4, pp. 54–60, 2002.
- [20] P. J. White and M. Yim, "Reliable external actuation for full reachability in robotic modular self-reconfiguration," *International Journal of Robotics Research (IJRR)*, vol. 29, no. 5, pp. 598–612, April 2010.
- [21] B. T. Kirby, B. Aksak, J. D. Campbell, J. F. Hoberg, T. C. Mowry, P. Pillai, and S. C. Goldstein, "A Modular Robotic System Using Magnetic Force Effectors," in *Intelligent Robots and Systems*, 2007, pp. 2787–2793.
- [22] K. Gilpin and D. Rus, "Modular robot systems: From self-assembly to self-disassembly," *Robotics and Automation Magazine*, vol. 17, no. 3, pp. 38–53, September 2010.
- [23] M. T. Tolley and H. Lipson, "On-line assembly planning for stochastically reconfigurable systems," *International Journal of Robotics Research (IJRR)*, vol. 30, no. 13, pp. 1566–1584, October 2011.
- [24] M. E. Karagozler, S. C. Goldstein, and J. R. Reid, "Stress-driven MEMS Assembly + Electrostatic Forces = 1mm Diameter Robot," in *Intelligent Robots and Systems*, 2009, pp. 2763–2769.
- [25] H. Kurokawa, "A geometric study of single gimbal control moment gyros," *Report of Mechanical Engineering Laboratory*, vol. 175, pp. 135–138, 1998.
- [26] B. Thornton, T. Ura, and Y. Nose, "Wind-up auvs: Combined energy storage and attitude control using control moment gyros," in *OCEANS*, 2007, pp. 1–9.
- [27] M. Gajamohan, M. Merz, I. Thommen, and R. D'Andrea, "The cubli: A cube that can jump up and balance," in *Intelligent Robots and Systems*, October, pp. 3722–3727.
- [28] N. M. Benbernou, "Geometric algorithms for reconfigurable structures," Ph.D. dissertation, Massachusetts Institute of Technology, 2011.